

Evidence of Soft Dipole Resonance in ^{11}Li with Isoscalar Character

R. Kanungo,¹ A. Sanetullaev,^{1,2} J. Tanaka,³ S. Ishimoto,⁴ G. Hagen,^{5,6} T. Myo,⁷ T. Suzuki,⁸ C. Andreoiu,⁹ P. Bender,² A. A. Chen,¹⁰ B. Davids,² J. Fallis,² J. P. Fortin,^{1,11} N. Galinski,² A. T. Gallant,² P. E. Garrett,¹² G. Hackman,² B. Hadinia,¹² G. Jansen,^{5,6} M. Keefe,¹ R. Krücken,^{2,13} J. Lighthall,² E. McNeice,¹⁰ D. Miller,² T. Otsuka,¹⁴ J. Purcell,¹ J. S. Randhawa,¹ T. Roger,¹⁵ A. Rojas,² H. Savajols,¹⁵ A. Shotter,¹⁶ I. Tanihata,^{3,17} I. J. Thompson,¹⁸ C. Unsworth,² P. Voss,⁹ and Z. Wang^{2,9}

¹Astronomy and Physics Department, Saint Mary's University, Halifax, Nova Scotia B3H 3C3, Canada

²TRIUMF, Vancouver, British Columbia V6T2A3, Canada

³RCNP, Osaka University, Mihogaoka, Ibaraki, Osaka 567 0047, Japan

⁴High Energy Accelerator Research Organization (KEK), Ibaraki 305-0801, Japan

⁵Physics Division, Oak Ridge National Laboratory, Oak Ridge, Tennessee 37831, USA

⁶Department of Physics and Astronomy, University of Tennessee, Knoxville, Tennessee 37996, USA

⁷General Education, Faculty of Engineering, Osaka Institute of Technology, Osaka, Osaka 535-8585, Japan

⁸Department of Physics, Nihon University, Setagaya-ku, Tokyo 156-8550, Japan

⁹Department of Chemistry, Simon Fraser University, Burnaby, British Columbia V5A 1S6, Canada

¹⁰Department of Physics and Astronomy, McMaster University, Hamilton, Ontario L8S 4M1, Canada

¹¹Department of Physics, University of Laval, Quebec City, Quebec G1V 0A8, Canada

¹²Department of Physics, University of Guelph, Guelph, Ontario N1G 2W1, Canada

¹³Department of Physics and Astronomy, University of British Columbia, Vancouver, British Columbia V6T 1Z1, Canada

¹⁴Department of Physics and Center of Nuclear Studies, University of Tokyo, Bunkyo-ku, Tokyo 113-0033, Japan

¹⁵Grand Accélérateur National d'Ions Lourds, CEA/DSM-CNRS/IN2P3, B.P. 55027, F-14076 Caen Cedex 5, France

¹⁶School of Physics and Astronomy, University of Edinburgh, EH9 3JZ, Edinburgh, United Kingdom

¹⁷School of Physics and Nuclear Energy Engineering and IRCPNC, Beihang University, Beijing 100191, China

¹⁸Lawrence Livermore National Laboratory, L-414, Livermore, California 94551, USA

(Received 24 December 2014; published 12 May 2015)

The first conclusive evidence of a dipole resonance in ^{11}Li having isoscalar character observed from inelastic scattering with a novel solid deuteron target is reported. The experiment was performed at the newly commissioned IRIS facility at TRIUMF. The results show a resonance peak at an excitation energy of 1.03 ± 0.03 MeV with a width of 0.51 ± 0.11 MeV (FWHM). The angular distribution is consistent with a dipole excitation in the distorted-wave Born approximation framework. The observed resonance energy together with shell model calculations show the first signature that the monopole tensor interaction is important in ^{11}Li . The first *ab initio* calculations in the coupled cluster framework are also presented.

DOI: 10.1103/PhysRevLett.114.192502

PACS numbers: 24.50.+g, 24.30.Gd, 25.45.De, 25.70.Ef

Nuclei with large neutron to proton asymmetry provide access to observe many unknown phenomena, among which a unique quantum system found was the Borromean halo nucleus. Here, two neutrons are weakly bound to a core nucleus and located at large distances from it, forming a low-density large neutron surface which is the neutron halo [1–3]. Since the discovery of the halo in ^{11}Li , it was first postulated that this extended density tail of the halo might give rise to a "soft electric dipole mode" [2]. Thereafter, a novel phenomenon was proposed whereby the oscillation of the halo neutrons and the core might lead to low-energy soft dipole resonance states [4]. Despite two decades of various experimental efforts, as mentioned in a recent review [5] it is yet to be established if indeed the very fragile two-neutron halo in ^{11}Li can sustain a soft dipole resonance state.

In this Letter, we report clear evidence of a soft dipole resonance state in ^{11}Li at 1.03 ± 0.03 MeV from a first measurement of the $d(^{11}\text{Li}, d')$ reaction. Deuterons being isoscalar probes, the peak observed has an isoscalar soft dipole resonance character.

This soft dipole resonance is a phenomenon occurring only when the nuclear surface has an appreciably large neutron-proton density difference. Therefore, it is different from the traditional term "pygmy dipole resonance" which was used to refer to resonances arising from nucleons outside an $N = Z$ core [6]. Studies in neutron-rich O, Ni, and Sn isotopes [5,7,8] reported some fragmentation of the dipole strength towards lower excitation energies (E_x) that are considered to be related to the neutron skin. However, these are still at fairly high E_x of ~ 10 MeV. Dipole resonances located slightly above the neutron threshold can have impact on the neutron capture rates in *r*-process nucleosynthesis [6,9].

Theoretical investigations of soft dipole states in medium heavy nuclei show that the degree of collectivity is more in the isoscalar dipole operator [10,11]. This large collectivity is due to the isoscalar reduced transition amplitude being predominantly determined by neutron particle-hole excitations, most of which add with the proton contributions. In a weakly bound halo nucleus like ^{11}Li , the dipole resonance states should be dramatically lowered in excitation energy

compared to the giant dipole resonance peak. There has been no identification so far of the isoscalar dipole resonance in ^{11}Li .

The pion double charge exchange reaction $^{11}\text{B}(\pi^-, \pi^+)^{11}\text{Li}$ [12] found indications of a peak at 1.2 ± 0.1 MeV. However, since this reaction does not favor the excitation of a collective state, and the dipole $L = 1$ nature was not established, it did not allow a firm conclusion on the soft dipole resonance. Proton inelastic scattering measurements reported a resonance peak at 1.3 ± 0.1 MeV with a width $\Gamma = 0.75 \pm 0.6$ MeV [13]. The poor resolution in the experiment, 2.2 MeV (FWHM), made it difficult to confirm the existence of a resonance state and define its properties. An analysis of the (p, p') data in the framework of multiple scattering expansion of the total transition amplitude [14] proposed that, while there is a strong dipole contribution, it is nonresonant in character. These calculations suggested an $L = 0$ resonance at an excitation energy of 0.5 MeV with a width $\Gamma = 0.6$ MeV. The pion capture reaction $^{14}\text{C}(\pi^-, pd)^{11}\text{Li}$ exhibited a peak at 1.02 ± 0.07 MeV [15], but this experiment did not allow a determination of the nature of the resonance or its width. Peaks were also found at $E_x = 2.07 \pm 0.12$ and 3.63 ± 0.13 MeV.

The $^{9}\text{Li}-n-n$ relative energy spectra from the different Coulomb dissociation measurements are not entirely consistent. The measurement at GSI [16] showed an enhancement around $E_x = 1.25$ MeV with C and Pb targets, while a second broad structure was seen around 2 MeV with a Pb target only. The measurement at MSU [17], on the other hand, showed an enhancement of the $E1$ strength peaked at $E_x \sim 1$ MeV. The most recent data from RIKEN [18] showed the dissociation spectrum with a Pb target peaked at a much lower $E_x \sim 0.6$ MeV.

The low-lying dipole strength observed from Coulomb dissociation in the one-neutron halo nucleus ^{11}Be has been understood to be of nonresonant character originating from the long tail of the halo wave function [19]. The $1/2^-$ excited state at 3.103 MeV [20] in ^{15}C is a dipole excitation but is not observed as a peak in the Coulomb dissociation spectrum [21]. These observations demonstrate that the Coulomb dissociation spectrum is dominated by nonresonant $E1$ strength associated with direct breakup from the halo density tail. Therefore, one needs studies through different experiments to investigate if the 0.6 MeV peak most recently observed in the Coulomb dissociation of ^{11}Li is a resonance state.

In order to conclusively establish a resonance in ^{11}Li and understand its nature, we performed the first measurement of deuteron inelastic scattering using a novel thin solid deuterium target. The experiment was performed at TRIUMF, Canada with the ^{11}Li beam reaccelerated to 5.5A MeV by using the superconducting linear accelerator at the ISACII facility. The study was undertaken using the newly developed ISAC charged particle spectroscopy station, IRIS [22], that is pioneering the use of a

windowless thin, $\sim 100 \mu\text{m}$, solid deuterium target. The experiment setup is shown in Fig. 1(a). The incoming ^{11}Li beam is counted throughout the experiment by using a low-pressure (19.5 Torr isobutane) ionization chamber. A total of $\sim 8 \times 10^8$ ^{11}Li bombarded the target with average intensity of ~ 3000 pps. The measured energy loss confirmed that the beam was devoid of isobaric contaminants. The beam then interacts with the solid D_2 target formed on a $5.4 \mu\text{m}$ Ag foil backing that faced the beam direction. A copper shield cooled to 30 K with an opening for the scattered particles surrounds the copper target cell (cooled to 4 K) to reduce the radiative heating. The targetlike reaction products, i.e., p, d, t , were identified [Fig. 1(b)] by using annular $\Delta E-E$ arrays of $100 \mu\text{m}$ thick segmented silicon detectors Si(YY1) followed by 12 mm thick CsI(Tl) detectors. The silicon detector array is composed of eight independent sectors forming an annulus and providing azimuthal segmentation. Each sector is segmented into 16 rings which provide the scattering angle. The detector array covered $\theta_{\text{lab}} = 32^\circ-58^\circ$. The CsI(Tl) array is segmented into 16 sectors where two sectors match one sector of the silicon detector. From the $\Delta E-E$ spectrum shown in Fig. 1(b), the scattered deuterons can be clearly identified. The energy and scattering angle of the deuterons is used to reconstruct the excitation energy spectra.

The heavy beam-like particles scattered at very forward angles pass through the hole in the annular Si(YY1)-CsI(Tl) array and are detected by using another $\Delta E-E$ array of double-sided silicon strip detectors. Each detector is segmented on one side into 24 rings which determine the scattering angle and on the reverse side into 32 azimuthal sectors. The ΔE layer is $60 \mu\text{m}$ thick, and the particles stop in the $500 \mu\text{m}$ thick

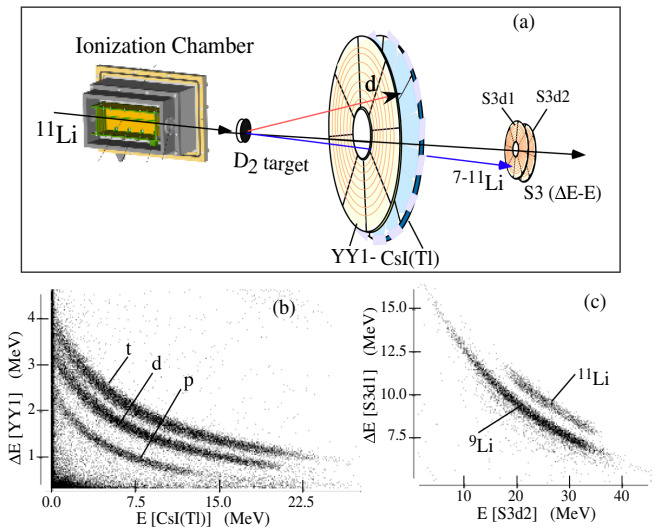


FIG. 1 (color online). (a) A schematic layout of the experiment. (b) Particle identification (PID) spectrum of light ejectiles using the Si(YY1)(ΔE) silicon array and the stopping (E) CsI(Tl) array. (c) PID spectrum of heavy reaction residues in coincidence with deuterons using the S3d1(ΔE) and the S3d2, stopping (E) silicon arrays.

E layer. For the events that are in coincidence with the deuterons detected by the Si(YY1)-CsI(Tl) array, the ΔE -*E* spectrum of the forward silicon telescope permits clear identification of the ${}^9,{}^{11}\text{Li}$ residues [Fig. 1(c)]. This detector array subtends laboratory angles ranging from $\theta_{\text{lab}} = 3.9^\circ$ to 12.3° . The forward silicon telescope also detects the peak position of ${}^{11}\text{Li}$ elastically scattered from the Ag backing foil. These data without and with the D_2 target are used to continuously determine the D_2 target thickness during the experiment. The target thickness was found to remain fairly constant over the period of the experiment.

The excitation energy of the ${}^{11}\text{Li}_{gs}$ deduced from the elastically scattered deuterons in coincidence with ${}^{11}\text{Li}$ yields a resolution of 700 keV (FWHM). The angular distribution from this coincident detection spans the center of mass scattering angle (θ_{cm}) range of 73° to 114° . The elastically scattered ${}^{11}\text{Li}$ identified by the forward silicon array alone extends the θ_{cm} coverage to 52° . Here the energy spectrum exhibits two distinct peaks due to scattering from the Ag foil and deuteron (d) that could be fitted by a sum of two Gaussians. The heat shield mask of the target limits the geometrical acceptance for deuteron detection, as it shadows parts of the Si(YY1)-CsI(Tl) telescope array. The detection efficiency was found both from the elastic scattering data as well as from simulation. A 5% uncertainty of the efficiency is taken for the simulation results, while the efficiency from the data has statistical uncertainties. The detection efficiency depends on angles covered and is shown in the inset in Fig. 2. The forward small silicon telescope within its angular coverage has full geometric efficiency for detecting the heavy particles, i.e., ${}^{11}\text{Li}$. The angular distribution is shown in Fig. 2. A consistency is found for the overlapping region where two different detection methods were used, namely, from deuteron- ${}^{11}\text{Li}$ coincidence (filled blue squares and open blue triangles) and ${}^{11}\text{Li}$ detection alone (filled red circles). This consistency establishes the correctness of the efficiency estimation. The coincident detection of d and ${}^{11}\text{Li}$ has negligible background under the elastic peak. The uncertainty in the cross section includes both statistical and systematic uncertainties. The statistical uncertainty also includes the uncertainties resulting from both the detection efficiency determination methods. Systematic uncertainties include the target thickness variation which was 15%. Data taken with Ag foil only (i.e., without the D_2) show a negligible nontarget background contribution to the deuterons in coincidence with ${}^{9,11}\text{Li}$.

A resonance state located above the two-neutron threshold of ${}^{11}\text{Li}$ at ~ 0.36 MeV will decay by neutron emission to ${}^9\text{Li}$. The inelastic scattering excitation energy spectrum is therefore obtained from a coincident detection of deuterons and ${}^9\text{Li}$. To reduce the nonresonant background, a condition is placed for the d and ${}^9\text{Li}$ to be in plane by requiring the azimuthal angle between them to be $180^\circ \pm 20^\circ$. The spectrum outside this range is a continuous background without any peak structure. The E_x spectrum in Fig. 3(a) shows a very prominent peak at 1.03 ± 0.03 MeV, which is also present

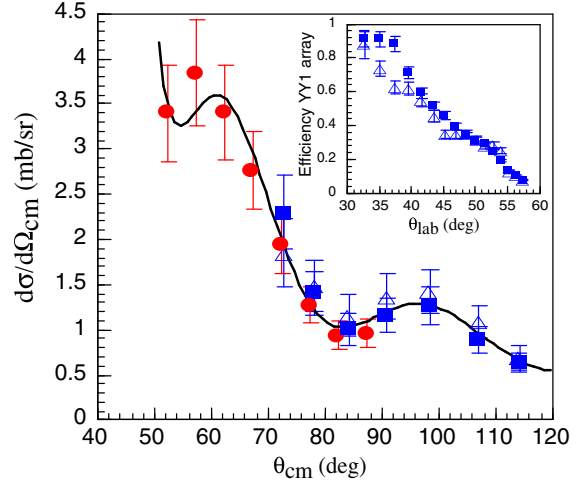


FIG. 2 (color online). Elastic scattering angular distribution for $d({}^{11}\text{Li}, d)$ at beam energy 55.3 MeV. The cross section with filled (blue) squares [open (blue) triangles] is from deuterons detected in the Si(YY1)-CsI(Tl) array by using efficiencies from simulation (elastic) data. The efficiency of the Si(YY1) array is shown in the inset, where filled squares are from simulation and open triangles are from elastic data. The cross section with filled red circles is from ${}^{11}\text{Li}$ detected in the S3 detector array. The curve shows distorted wave Born approximation (DWBA) predictions.

without the in-plane condition. The width of this resonance was found to be 0.51 ± 0.11 MeV (FWHM). This width is obtained from a fit to the data with either a Gaussian or a Breit-Wigner distribution with an energy-independent width folded by the Gaussian experimental resolution (FWHM ~ 700 keV from elastic scattering) together with an exponential background. The limited statistics do not allow for meaningful consideration of a potential asymmetry. The broad structure around 3.5 MeV is not statistically significant for distinguishing between phase space effects and resonance peak. Hence we do not discuss any further on that. In order to obtain the differential cross section [Fig. 3(b)], the spectrum for $E_x < 3.5$ MeV is fitted with an exponential background [Fig. 3(a), inset]. The background-subtracted counts under the 3σ Gaussian peak region were taken. Other background estimates using a linear function or a second Gaussian peaked around 3.5 MeV did not affect the shape of the angular distribution but cause a variation in the overall magnitude which is included in the systematic uncertainty. Only the statistical uncertainty is shown in Fig. 3(b), since our aim is to determine the shape of the angular distribution. The systematic uncertainties contribute an additional 30%.

The angular distributions are interpreted in the framework of a one-step distorted wave Born approximation calculation using the code FRESCO [23]. The calculated elastic scattering angular distribution (black curve in Fig. 2) yields the best fit optical potential parameters. By using these potential parameters and a collective form factor, the inelastic scattering angular distribution is calculated for $L = 0, 1$, and 2 as possible multipolarities of excitation from the ${}^{11}\text{Li}_{gs}$ to the

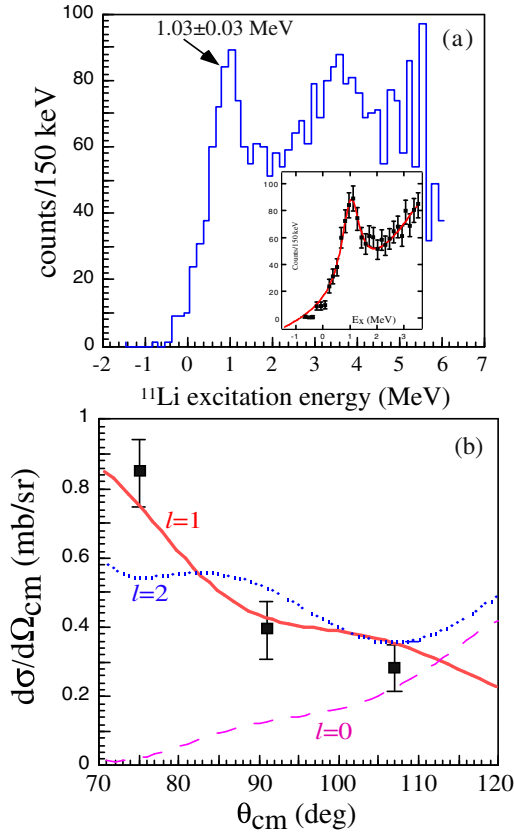


FIG. 3 (color online). (a) Inelastic scattering excitation energy spectrum for deuterons in coincidence with ${}^9\text{Li}$. (b) The inelastic scattering angular distribution data for the resonance peak at $E_{ex} = 1.03$ MeV. The curves are DWBA calculations for $L = 0$ (pink dashed line), $L = 1$ (red solid line), and $L = 2$ (blue dotted line).

1.03 MeV excited state. Figure 3(b) shows that the angular distribution normalized to the data is consistent with an $L = 1$ excitation, thereby establishing the dipole character of the resonance state. The minimum χ^2 for $L = 0$ and 2 distributions are more than 2 standard deviations higher than that for $L = 1$. Deuteron inelastic scattering will excite only isoscalar dipole resonance(s), since the deuteron is an isoscalar probe ($T = 0$). Therefore, this observation provides the first clear evidence of the isoscalar soft dipole excitation character of this resonance state. The vibration of the halo neutrons against the core is associated to an in-phase vibration of core protons and neutrons giving rise to the isoscalar dipole mode. A dipole transition opens the possibility of the resonance state having a spin of $1/2^+$, $3/2^+$, or $5/2^+$.

Figure 4 compares various theoretical predictions with the data. The first predictions based on a hybrid model by Ikeda [4] is shown as model 11. The lowest resonance is quite close to the data, but as discussed in Ref. [4] improvements in this model are needed for a more realistic comparison to the experiment. In this Letter, we present three new calculations that are discussed below.

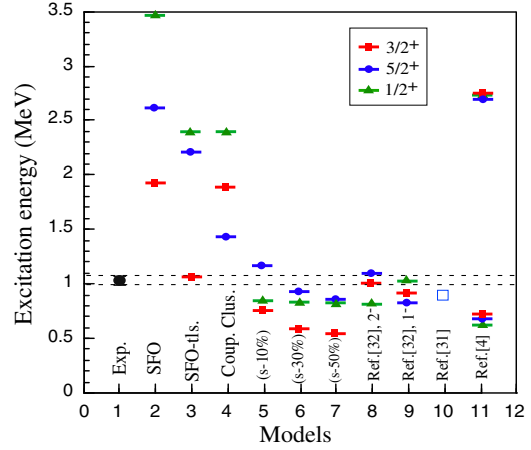


FIG. 4 (color online). The experimental excitation energy compared with different theoretical model predictions: (1) experimental data; shell model with (2) SFO and (3) SFO-tls interactions; (4) coupled cluster; (5)–(7) three-body model with $2s_{1/2}$, 10%, 30%, and 50%, respectively; (8) Ref. [24] with ${}^{10}\text{Li}(2^-)$; (9) Ref. [24] with ${}^{10}\text{Li}(1^-)$; (10) Ref. [25]; and (11) Ref. [4]. The red (squares), blue (circles), and green (triangles) lines represent states with spin $3/2^+$, $5/2^+$, and $1/2^+$, respectively.

Shell model calculations with dipole operators were performed by using the SFO [26] and SFO-tls [27] interactions with p - sd configurations including up to $3\hbar\omega$ excitations. The SFO-tls interaction with the single particle energy of the s orbital lowered to match the ${}^{11}\text{Be}$ levels is used. The probabilities for p^2 - and sd^2 (s^2)-shell configurations in ${}^{11}\text{Li}$ are 38.9% and 61.1% (33.6%), respectively, for the SFO interaction. The SFO-tls interaction leads to the configuration components of 56.1% and 43.4% (21.7%), respectively. The p -shell part of the SFO Hamiltonian is obtained from the Cohen-Kurath Hamiltonian [28], and the $p - sd$ part is from the Millener-Kurath interaction [29]. The SFO-tls interaction has an improved spin-orbit and tensor component in the p - sd cross-shell part that is consistent with the $\pi + \rho$ meson exchange potential. This leads to an enlarged tensor component. Figure 4 shows that differences between the SFO (model 2) and SFO-tls (model 3) interactions have significant impact on the energy of the dipole resonances. The larger tensor and spin-orbit contribution in SFO-tls greatly lowers the excitation energy. The result of the SFO-tls interaction (Fig. 4, model 3) for the lowest resonance is found to be in good agreement with the experimental data, thereby showing the importance of the monopole part of tensor interaction in ${}^{11}\text{Li}$.

In another framework, the ${}^{11}\text{Li}$ nucleus is described with the ${}^9\text{Li} + n + n$ three-body model. An inert ${}^9\text{Li}$ core plus two halo neutrons with an isovector dipole transition operator predicts low-lying dipole resonances. The results are shown in Fig. 4 (models 5–7). The excitation energies of the $3/2^+$ and $5/2^+$ dipole resonances are predicted to have a strong dependence on the s^2 component in the wave function of ${}^{11}\text{Li}$. On the other hand, in the tensor-optimized shell model

(TOSM) [30,31], the tensor correlation in ${}^9\text{Li}$ is variationally treated by including the high momentum component of $2p2h$ states in the configuration mixings. This model produces the Pauli-blocking effect on the p -shell configuration of ${}^{11}\text{Li}$, which dynamically enhances the s -wave mixing probability of last two neutrons in ${}^{11}\text{Li}$ and explains the ground state properties. The dipole excitation within the TOSM framework was also studied in this work; however, no low-lying dipole resonances were predicted. This may point towards the necessity to include excited ${}^9\text{Li}$ core components in the TOSM model.

In a first effort to investigate ${}^{11}\text{Li}$ in an *ab initio* framework, coupled cluster calculations including the chiral next-to-next-to-leading order (NNLO) force [32] with the two-nucleon interaction only were performed. The states of ${}^{11}\text{Li}$ were computed as a proton attached to the ${}^{10}\text{He}$ ground state where the two last neutrons fill up the $2s_{1/2}$ orbital. Up to $3p-2h$ excitations were considered. In this approach, instead of using a dipole operator, the spin of the states determines the dipole excitation. The results are shown in Fig. 4 (model 4). The excitation energy is higher than the data, and the spin ordering of the $3/2^+$ and $5/2^+$ levels is inverted compared with the shell model results. Further developments including continuum effects and three-nucleon force will be investigated in the future.

The Coulomb breakup of ${}^{11}\text{Li}$ studied in a three-body model [25] predicts a narrow 1^- resonance at 0.5 MeV above the two-neutron threshold (i.e., $E_x \sim 0.86$ MeV). The predicted excited state (Fig. 4, model 10) is in moderate agreement, being slightly below the 1σ error of the data. However, unlike the conclusion presented in Ref. [25], the present data clearly confirm that the low-lying resonance in ${}^{11}\text{Li}$ is not consistent with the peak in the Coulomb breakup. Dipole resonances in ${}^{11}\text{Li}$ have also been investigated in a complex scaling method [24] (Fig. 4, models 8 and 9). The results depend on the ${}^{10}\text{Li}$ resonances, model 8 and 9 for 2^- and 1^- ground states, respectively, of ${}^{10}\text{Li}$ and are in fairly good agreement with the data. From Fig. 4, we see that the three-body models 5–10 predict closely spaced resonances around 1 MeV, which is different from the shell model and coupled cluster model predictions. However, most of the models show the presence of a low-energy dipole state.

In summary, the first measurement of $d({}^{11}\text{Li}, d')$ inelastic scattering provides firm evidence for the existence of a soft dipole resonance at $E_x = 1.03 \pm 0.03$ MeV with a width (FWHM) of 0.51 ± 0.11 MeV having isoscalar character. The excitation energy compared to shell model predictions shows the first signature of the importance of the monopole component of the tensor force in ${}^{11}\text{Li}$. Three-body models of ${}^{11}\text{Li}$ also predict resonances close to the data. The first coupled cluster calculations with two-nucleon force show resonances at somewhat higher energies than observed. The present data suggest that the peak observed in Coulomb dissociation is a nonresonant enhancement from direct breakup.

The authors express sincere thanks to the TRIUMF beam delivery team. The support from Canada Foundation for Innovation, NSERC, Nova Scotia Research and Innovation Trust is gratefully acknowledged. This work is supported by the grant-in-aid program of the Japanese government under Contract No. 23224008. This work was performed under the auspices of the U.S. Department of Energy by Lawrence Livermore National Laboratory under Contract No. DE-AC52-07NA27344. Discussions with T. Papenbrock are gratefully acknowledged.

- [1] I. Tanihata, H. Hamagaki, O. Hashimoto, Y. Shida, N. Yoshikawa, K. Sugimoto, O. Yamakawa, T. Kobayashi, and N. Takahashi, *Phys. Rev. Lett.* **55**, 2676 (1985).
- [2] P. G. Hansen and B. Jonson, *Europhys. Lett.* **4**, 409 (1987).
- [3] I. Tanihata, H. Savajols, and R. Kanungo, *Prog. Part. Nucl. Phys.* **68**, 215 (2013).
- [4] K. Ikeda, *Nucl. Phys.* **A538**, 355c (1992).
- [5] D. Savran, T. Aumann, and A. Zilges, *Prog. Part. Nucl. Phys.* **70**, 210 (2013).
- [6] J. S. Brzosko, E. Gierlik, A. Soltan Jr., and Z. Wilhelm, *Can. J. Phys.* **47**, 2849 (1969).
- [7] P. Adrich *et al.*, *Phys. Rev. Lett.* **95**, 132501 (2005).
- [8] D. Rossi *et al.*, *Phys. Rev. Lett.* **111**, 242503 (2013).
- [9] S. Goriely, *Phys. Lett. B* **436**, 10 (1998).
- [10] X. Roca-Maza, G. Pozzi, M. Brenna, K. Mizuyama, and G. Colo, *Phys. Rev. C* **85**, 024601 (2012).
- [11] D. Vretenar, Y. F. Niu, N. Paar, and J. Meng, *Phys. Rev. C* **85**, 044317 (2012).
- [12] T. Kobayashi *et al.*, *Nucl. Phys.* **A538**, 343c (1992).
- [13] A. A. Korsheninnikov *et al.*, *Phys. Rev. Lett.* **78**, 2317 (1997).
- [14] R. Crespo, I. J. Thompson, and A. A. Korsheninnikov, *Phys. Rev. C* **66**, 021002(R) (2002).
- [15] M. G. Gornov, Y. Gurov, S. Lapushkin, P. Morokhov, V. Pechkurov, T. K. Pedlar, K. K. Seth, J. Wise, and D. Zhao, *Phys. Rev. Lett.* **81**, 4325 (1998).
- [16] M. Zinser *et al.*, *Nucl. Phys.* **A619**, 151 (1997).
- [17] K. Ieki *et al.*, *Phys. Rev. Lett.* **70**, 730 (1993).
- [18] T. Nakamura *et al.*, *Phys. Rev. Lett.* **96**, 252502 (2006).
- [19] N. Fukuda *et al.*, *Phys. Rev. C* **70**, 054606 (2004).
- [20] F. Ajzenberg-Selove, *Nucl. Phys.* **A523**, 1 (1991).
- [21] U. Datta-Pramanik *et al.*, *Phys. Lett. B* **551**, 63 (2003).
- [22] R. Kanungo, *Hyperfine Interact.* **225**, 235 (2014).
- [23] I. J. Thompson, *Comput. Phys. Rep.* **7**, 167 (1988).
- [24] E. Garrido, D. V. Fedorov, and A. S. Jensen, *Nucl. Phys.* **A722**, C221 (2003).
- [25] E. C. Pinilla, P. Descouvemont, and D. Baye, *Phys. Rev. C* **85**, 054610 (2012).
- [26] T. Suzuki, R. Fujimoto, and T. Otsuka, *Phys. Rev. C* **67**, 044302 (2003).
- [27] T. Suzuki and T. Otsuka, *Phys. Rev. C* **78**, 061301(R) (2008).
- [28] S. Cohen and D. Kurath, *Nucl. Phys.* **73**, 1 (1965).
- [29] D. J. Millener and D. Kurath, *Nucl. Phys.* **A255**, 315 (1975).
- [30] T. Myo, K. Kato, H. Toki, and K. Ikeda, *Phys. Rev. C* **76**, 024305 (2007).
- [31] T. Myo, A. Umeya, H. Toki, and K. Ikeda, *Phys. Rev. C* **86**, 024318 (2012).
- [32] A. Ekstrom *et al.*, *Phys. Rev. Lett.* **110**, 192502 (2013).